Multiple charge density wave transitions in $Lu_2Ir_3Si_5$ single crystal

N. S. Sangeetha[1], A. Thamizhavel[2], C. V. Tomy[3], Saurabh Basu[1], A. M. Awasthi[4], S. Ramakrishnan[2] and D. Pal[1*]
[1]*Department of Physics, Indian Institute of Technology Guwahati, Guwahati, Assam-781039, India*
[2]*Department of Condensed Matter Physics and Materials Science, Tata Institute of Fundamental Research, Homi Bhabha Road, Colaba, Mumbai-400 005, India*
[3]*Department of Physics, Indian Institute of Technology Bombay, Mumbai - 400076, India and*
[4]*IUC-DAEF, Indore-452017, India*
(Dated: September 5, 2018)

The physical properties of the single-crystalline samples of $Lu_2Ir_3Si_5$ have been investigated by magnetic susceptibility, resistivity and heat capacity studies. We observed multiple charge density wave (CDW) transitions in all the measurements. A strong thermal hysteresis at these transitions suggests a possible first order CDW ordering. In addition, the first order nature is ascertained by a very narrow and a huge cusp (62 J/mol K) in the zero field specific heat data which also suggests a strong interchain coupling. By applying a field of 9T in the specific heat measurement, one of the CDW transitions is suppressed.

I. INTRODUCTION

Charge-density-wave (CDW) transitions expected to occur in low dimensional solids where it is possible to achieve nesting of Fermi surfaces that leads to the appearance of a periodic lattice distortion with an accompanying energy gap. The instability to achieve the instability in low dimensional solids was first demonstrated by Pierels[1,2]. This is very well documented from the early works of many research groups performed on a wide range of quasi-low-dimensional systems includes transition-metal dichalcogenides and trichalcogenides[3–6]. Even though in three-dimensional (3D) compounds it is not possible to get a perfect nesting but CDW ordering has also been established in 3D materials such as $R_2Ir_3Si_5$[8] and $R_5Ir_4Si_{10}$[9] (R = rare-earth elements). So it appears that even in the presence of imperfect nesting there remains a possibility for the appearance of a CDW. In order to understand the nature of such novel CDW in such systems, a further search for new classes of materials are needed.

Recently reported $R_5Ir_4Si_{10}$ (R=Dy-Lu) compounds exhibit strong coupling CDW at high temperatures accompanying with superconductivity or magnetic ordering at low temperature[10]. Interestingly, the multiple CDW anomalies were observed in Dy, Ho, Er and Tm[11]. The compound $Lu_5Ir_4Si_{10}$ shows the coexistence of superconductivity and strongly coupled CDW transition[12]. From the literature, it is found that the compound $R_5Ir_4Si_{10}$ presents a complex 3D structure with several substructures such as one-dimensional R chains and 3D cages in which a variety of many-body effects (superconductivity and magnetism) originate. Similar complex behavior has recently reported in $R_2Ir_3Si_5$ system, which display various unusual ground states like, superconductivity, CDW, Kondo behavior, coexistence of CDW and superconductivity or magnetism, etc .

In $R_2Ir_3Si_5$ series, the compound $Lu_2Ir_3Si_5$ is of special interest, as it exhibits superconductivity at 3.5 K and shows strongly coupled first order CDW transition between 150 and 200 K.[13]. Kuo *et al.* recently reported the possibility for the CDW transition accompanying with a similar structural phase transition followed by the transport measurements[14]. Besides, in our earlier work, we have reported a non-monotonicity of the transition temperatures, T_{CDW} and T_{SC} as a function of Ge substitution[15]. This study revealed the complex nature of the CDW ordering such that the system may undergoes coexistence/mixture of multiple phase CDW ordering with the suppression of CDW upto certain Ge concentration afterwards a sudden enhancement of it. Definite understanding of this feature needs further experimentation on single crystal of $Lu_2Ir_3Si_5$. In this paper we provide an observation of multiple CDW transitions in $Lu_2Ir_3Si_5$ single crystals using thermodynamic, transport and magnetic measurements.

II. EXPERIMENT

Two single-crystalline samples of $Lu_2Ir_3Si_5$ were grown in a tetra-arc furnace using a modified Czochralski technique. The purity of the elements, melted in a stoichiometric ratio, were Lu: 99.999%; Ir: 99.99%; Si: 99.999%. The samples were characterized using scanning electron microscopy equipped with energy-dispersive X-ray analysis (EDAX) to prove its 2-3-5 stoichiometry. The room temperature powder x-ray diffraction with Cu Kα radiation was taken on the samples by using PANalytical commercial X-ray diffractometer. A commercial superconducting quantum interference device (SQUID) magnetometer (MPMS5, Quantum Design, USA) was used to measure dc magnetic susceptibility as a function of temperature between 100 and 300 K. The electrical resistivity between 1.8 and 300 K was measured by using a home built electrical resistivity set up with the standard dc four probe technique. The specific heat data were taken on the samples for the temperature range 120 to 300 K in zero field, by using a DSC set up, and in 9 T field by using a commercial physical property measurement system (PPMS, Quantum Design, USA). The reproducibility of the results was checked by repeating

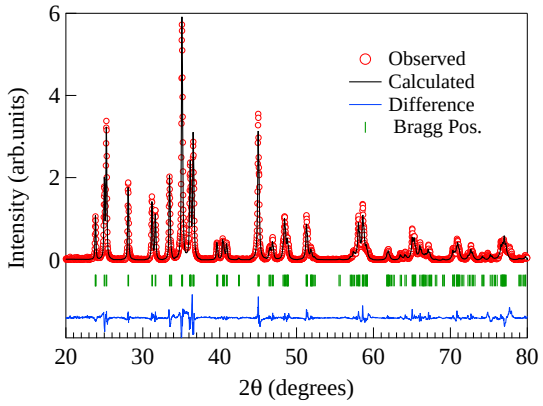

FIG. 1: (color line) Powder X-ray diffraction data of the $Lu_2Ir_3Si_5$ at 300 K. The solid line is the simulated data using the FulProf (Reitveld Program).

the measurements on the same samples.

III. RESULTS

A. X-ray diffraction studies

The powder X-ray diffraction pattern of $Lu_2Ir_3Si_5$ at 300 K clearly reveals the absence of any impurity phase and also confirms that the samples have a $U_2Co_3Si_5$ - orthorhombic type structure with the space group *Ibam*. The Fullprof Reitveld fit[16] to the powder x-ray data of $Lu_2Ir_3Si_5$ is shown in Fig. 1. The extracted lattice parameters from this fit are $a = 9.923 \pm 0.0005$ÃĚ, $b = 11.311 \pm 0.0005$ÃĚ and $c = 5.732 \pm 0.0005$ÃĚ which are in close agreement with the previously reported polycrystalline data[13]. The single crystalline nature of the samples was verified by Laue diffraction technique. The single crystals were oriented along three principle crystallographic directions, which are mutually perpendicular to each other, by using back-reflection Laue diffraction method. The observed Laue pattern of each direction was analyzed, with the simulated pattern, by using Orient Express software. The observed Laue pattern of an oriented crystal, along [100] direction, is shown in Fig. 2. For transport and magnetization measurements, small bars (required size) were cut by spark erosion from the oriented crystals.

Fig. 3 depicts the unit cell of $Lu_2Ir_3Si_5$ crystal structure. One observes the absence of transition metal (Ir-Ir) contacts. The Ir-Si-Ir bond is formed as a cage around Lu atom which is stacked along the *ab* plane, shown in Fig. 3(a). The Lu atoms form a quasi one - dimensional (1D) zig-zag chain along the *c*-axis (Fig. 3(a)) which are well separated from the Ir-Si ring. It can be found, in Fig. 3(b), that the zig-zag chain of Lu atom is strongly coupled with the *b*-axis through Ir1 atom. By analyzing the distances between other atoms, these Lu atoms have the shortest distance with respect to all other bonds; suggesting a quasi-1D conducting channel in the Lu - Lu chain, developing along the *c*-axis.

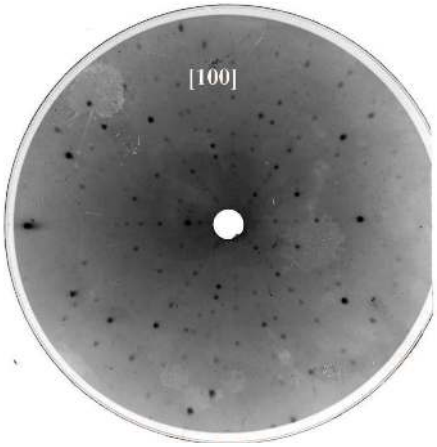

FIG. 2: The observed Laue pattern of $Lu_2Ir_3Si_5$ along [100] axis.

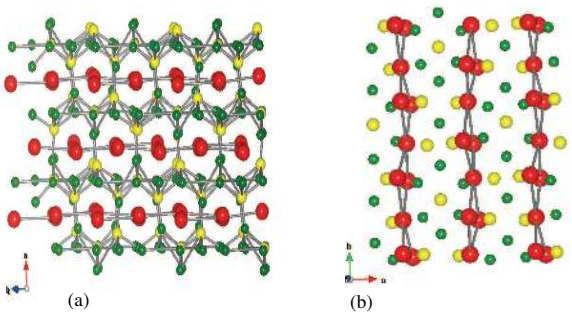

FIG. 3: (Color online) The crystal structure of $Lu_2Ir_3Si_5$. The large (red) spheres are correspond to Lu atom, Ir atoms with medium (yellow) spheres and Si atoms with small (green) spheres.

B. Electrical resistivity

Fig. 4 shows the temperature dependent resistivity of $Lu_2Ir_3Si_5$ along *a, b* and *c* axes. In this Figure, the inset of the left panel shows $\rho(T)$ taken during cooling and warming cycles, between 140 and 300 K, at the rate of 1 K/min. $\rho(T)$ exhibits a sharp upturn between 170 and 250 K, while cooling and warming cycles, signifies the opening up of a gap in the electronic density of states at the Fermi surface. This behavior is similar to the one usually observed in charge-density wave (CDW) transition.During the cooling cycle the upturn of $\rho(T)$, related to CDW transition, starts at ∼210 K and reaches a maximum at ∼175 K. While in the warming cycle, the maximum of $\rho(T)$ occurs at ∼215 K then it decreases sharply and exhibits minimum at∼250 K.

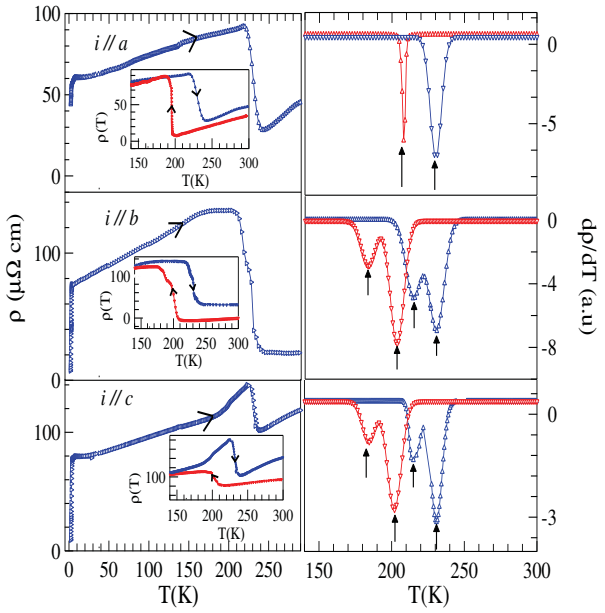

FIG. 4: (color online) The temperature dependence of the electrical resistivity $\rho(T)$ of $Lu_2Ir_3Si_5$. Left panel shows the resistivity for temperature scans between 1.8 to 300 K. The inset of left panel shows $\rho(T)$ illustrating the hysteresis between 140 and 300 K in the resistivity taken on cooling (red triangle) and warming (blue triangle) cycle for $Lu_2Ir_3Si_5$ along the *a, b* and *c* axes. Right panel shows $d\rho/dT$ as a function of temperature between 140 and 300 K highlights multiple anomalies. The solid arrows indicate the transition temperatures of the anomalies.

axis	Resistivity T_{CDW} (K)		Susceptibility T_{CDW} (K)	
	Cooling	warming	Cooling	warming
a	197	231	199	232
b	184 200	213 232	181 201	214 231
c	184 202	215 231	183 204	212 230

TABLE I: CDW transition temperatures T_{CDW} observed from both resistivity and susceptibility measurement techniques.

As a result of these CDW transitions, a large hysteresis of almost 40-50 K is associated between the up and down scans. This strongly suggests a first-order CDW transition for the system. Besides, we can see in the figure that the transition is rather broad one at around 35 K. Such a broad curvature and an unusually large upward jump seen in the resistivity data with a step like increase (with decreasing temperature) across the transition signifies the mixture of multiple CDW phase in the sample (seen in Fig 4) as were observed in $Er_5Ir_4Si_{10}$[17]. In order to have a better understanding of CDW transitions, The derivative of resistivity ($d\rho/dT$ *vs* T) is also plotted against temperature (shown in right panel of Fig. 4). From this, one can clearly elucidate the presence of multiple transitions for cooling and warming the sample along *b* and *c* axes. The anomalies are marked with solid arrows. It must be noted that there is no second anomaly along the *a*-axis. We shall return to this point as we discuss further. The characterized CDW transition temperatures T_{CDW} obtained from resistivity measurement is listed in Table I.

C. Magnetic susceptibility

Fig. 5 shows dc magnetic susceptibility and its derivative of $Lu_2Ir_3Si_5$, as a function of temperature from 150 to 300 K, with an applied magnetic field $H = 5$T along *a*, *b* and *c* axes.

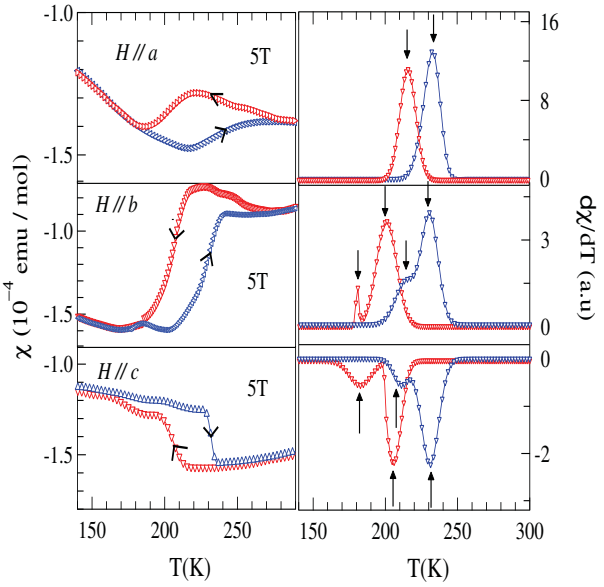

FIG. 5: The temperature dependence of the dc susceptibility $\chi(T)$ of $Lu_2Ir_3Si_5$. Left panel demonstrates dc susceptibility in the temperature range between 140 and 300 K to highlights CDW transition along three principle axes (*a*, *b* and *c*) for both cooling (red triangle) and warming (blue triangle) the sample, its corresponding derivatives plots are shown in the right panel of the figure.

The magnetic susceptibility data (shown in the left panel) show a large diamagnetic drop across the phase transition at around 250 K and 170 K during warming and cooling the sample respectively. This comes about due to the reduction in the density of states at the Fermi surface because of the opening up of a gap at the Fermi

surface, accompanying the CDW ordering. A huge thermal hysteresis (40-50 K) associated with the CDW ordering along the three axes, as observed in our resistivity results, signifies a first-order characteristic of CDW transition. The derivative plots of susceptibility ($d\chi/dT$ *vs* T), shown in the right panel of Fig. 5, demonstrate multiple CDW anomalies for b and c axes which are marked by solid arrows. The broad anomalies of susceptibility data also corroborate the above inference. Concurrently, one can see a single peak along the a axis as found in resistivity data. In contrast, there is an enhancement of magnetization across the CDW transition along the c axis. We will return to this point later in the discussion part. The CDW transition temperature obtained from the susceptibility studies, listed in Table I, are in good agreement with the above mentioned resistivity results.

D. Heat capacity

Fig. 6 shows the zero field specific heat data for $Lu_2Ir_3Si_5$ in the temperature range between 150 and 300 K. The background subtraction of specific heat is done by fitting the lattice contribution of specific heat, for the data far away from the transition, to demonstrate the heat capacity jumps, $\triangle C_{CDW}$. The entropy change $\triangle S_{CDW}$ across the CDW transition is obtained by integrating the curve under $\triangle C_{CDW}/T$ as a function of T. The transition temperature T_{CDW}, heat capacity jumps $\triangle C_{CDW}$ and the entropy change $\triangle S$ during warming and cooling the sample (seen in Fig. 6) are listed in Table II.

	T_{CDW} (K)	Total $\triangle C_{CDW}$ (J/ mol K)	Total $\triangle S$(R)
warming curve	218 K 232 K	62	0.42
cooling curve	185 K 198 K	62	0.42

TABLE II: The parameters obtained from heat capacity studies of $Lu_2Ir_3Si_5$.

The values of transition temperatures are in good agreement with both susceptibility and resistivity results. It has been observed that the specific heat anomaly and the entropy change for $Lu_2Ir_3Si_5$ single crystal are much larger and sharper than that of conventional CDW systems such as $K_{0.3}MoO_3$ (8 J/mol K, $0.18R$)[18–20] and $NbSe_3$ ($\sim$9 J/mol K, $0.08R$)[21].

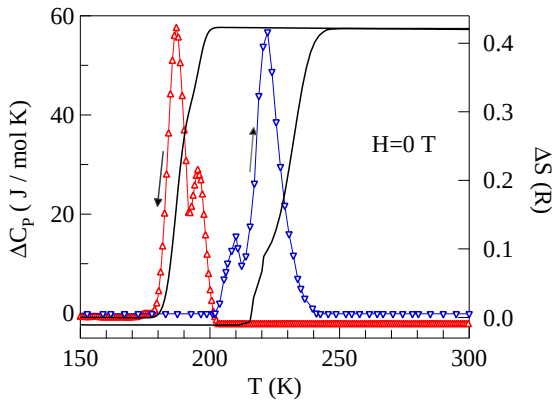

FIG. 6: The temperature dependence of specific heat measurements $\triangle C_P$ *vs* T (left axis) on both warming (blue triangle) and cooling (red triangle) of $Lu_2Ir_3Si_5$ after subtracting the smooth background. Entropy $\triangle S$ associated with the transition is estimated after background substraction, shown in right axis of the plot.

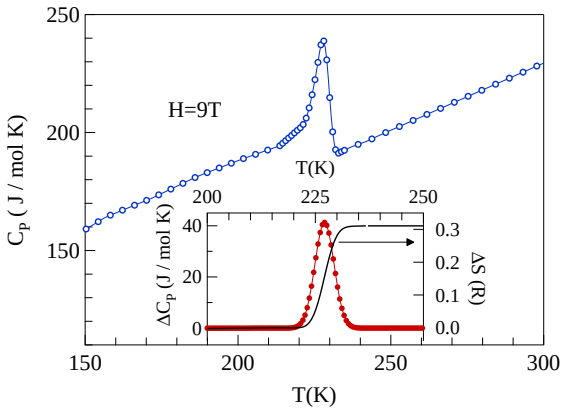

FIG. 7: The specific heat capacities of $Lu_2Ir_3Si_5$in the field of 9 T while warming the sample from 150 to 300 K. Inset shows the specific heat (left axis) on an enlarged temperature scale and the calculated entropy change (right axis) between 200 and 250 K .

The presence of a sharp peak anomaly in the specific heat data gives the clear evidence of a high electron density and a large amplitude of the periodic lattice distortion accompanying the CDW. Compared to the 2H-$TaSe_2$ and 2H-TaS_2 layered compounds[22], this large phonon specific heat anomaly may be due to the presence of an incommensurate CDW phase. The huge cusp in heat capacity data ($\triangle C_{CDW}$=62 J/mol K) and the pronounced thermal hysteresis, in the warm up and cooling down scans, are the characteristic features expected in a strongly coupled first order CDW transition. The additional peaks observed at 218 K and at 186 K in the heating and cooling curves, respectively, (shown in Fig. 6) indicate the mixture of multiple CDW transition in the compound. These findings are well consistent with the

above mentioned resistivity and susceptibility studies.

Fig. 7 demonstrates the heat capacity data between 150 and 300 K performed in PPMS set up by applying a magnetic field of 9 T. A huge peak ($\triangle C_P$ is 42 J/mol K) is observed at 232 K, while no anomaly is found at lower transition 218 K. The sharp ($\triangle T_{_{CDW}}/T_{_{CDW}} \sim 3\%$) upper transition is accompanied by an entropy change of $0.32R$, where R is a gas constant.

IV. DISCUSSION

In this section, we will discuss the possible origin of multiple CDW transitions observed in $Lu_2Ir_3Si_5$ single crystal. In this context it is worthwhile to recapitulate multiple CDW transitions observed in other materials. In the layered compound $NbSe_3$ which shows a two dimensional structure, there are reports of two CDW transitions occurring at 145 and 49 K[23]. The transition at 145 K is related to the rearrangement of the atoms in the four-chain units resulting in the appearance of the CDW phase. Similarly the transition at 49 K is related to the two-chain units in the *bc* plane of the crystal. Hence, the two CDW would have different wavelengths and their formation would take place at different temperatures and they are not correlated. So in $NbSe_3$, it requires two independent Fermi nesting conditions for the development of two CDW anomalies. Multiple CDW transitions is also reported in a few of the $R_5Ir_4Si_{10}$ (R=rare earth) compounds[11]. In these compounds, one of the rare earth atoms forms a chain-like structure along the c - axis resulting in the formation of a quasi 1D chain. The rearrangement of this quasi 1D chain results in the formation of a CDW phase. It is observed that in these materials the low temperature purely commensurate CDW phase is achieved via a 1D incommensurate CDW phase transition at high temperatures. This is endorsed by superlattice reflections at various temperatures. However this multiple CDW ordering is not observed in $Lu_5Ir_4Si_{10}$.

We have demonstrated that $Lu_2Ir_3Si_5$ exhibits the multiple first order CDW transition by the resistivity, susceptibility and specific heat measurement. By looking the crystal structure of $Lu_2Ir_3Si_5$, (ref. Fig. 3), it can be safely assumed that the CDW anomalies is related to the quasi 1D chain of Lu atoms along the c - axis. Hence we speculate that this Lu chain of atoms might be rearranging themselves twice via commensurate/incommensurate modes, resulting in appearance of multiple CDW phases. Synchrotron measurements are needed to confirm this. Such multiple transitions is favourable to be observed along b and c axis as this compound has the zig-zag chain of Lu atoms spread over bc plane.

Interestingly, the susceptibility data along the c-axis shows an upward jump across the CDW ordering whereas it shows a drop in susceptibility along the $a$and b axes. This means that the DOS along the c-axis reduces whereas along a and b axes it enhances across the transition. Such an effect was earlier observed in $Tm_5Ir_4Si_{10}$[11]. We speculate that Lu atoms play a definite role in these transitions and further understanding requires band structure calculations to determine the possible nesting and gaping of the FS.

V. CONCLUSION

To conclude, the detailed bulk measurements suggest the multiple CDW anomalies in $Lu_2Ir_3Si_5$ single crystal. In addition, a large thermal hysteresis of about 50 K has been observed in magnetic susceptibility, electrical resistivity, and heat capacity measurements across the CDW ordering which suggests a first order phase transition associated with incommensurate CDW transition. Besides, the giant excess of specific heat $\triangle C_P/C_P \sim 26\%$ and the huge specific heat jump (62 J/mol K) further support the strong coupling first order CDW scenario. However, definite conclusion of aforesaid scenarios need further experimentation on $Lu_2Ir_3Si_5$, concerning structural fluctuation and lattice softening (inelastic neutron scattering). Synchrotron X-ray study of the system is to be performed to determine q vectors for the CDW transition.

VI. ACKNOWLEDGMENT

N.S.S. thank to Prof. A. K. Grover, TIFR Mumbai, for his various kind of support throughout the current research work. N.S.S. also grateful to Bhanu Joshi for his help during the experiments. C. V. Tomy would like to acknowledge the Department of Science and Technology for the partial support of this work.

* Electronic address: dpal@iitg.ernet.in

[1] R. E. Peierls, *Quantum Theory of Solids* (Oxford University Press, New York, 1955).
[2] G. Gruner, *Density Waves in Solids* (Addison-Wesley, Reading, 1994).
[3] L. Degiorgi, B. Alavi, G. Mihaly, and G. Gruner, Phys. Rev. B **44**, 7808 (1991).
[4] S. Sridhar, D. Reagor, and G. Gruner, Phys. Rev. Lett. **55**, 1196 (1985).
[5] T. Giamarchi, S. Biermann, A. Georges, and A. Lichtenstein, J. Phys. IV France **114**, 23 (2004).
[6] A. Schwartz, M. Dressel, G. Gruner, V. Vescoli, L. Degiorgi, and T. Giamarchi, Phys. Rev. B **58**, 1261 (1998).
[7] [34]. M. Kumar, V. K. Anand, C. Geibel, M. Nicklas and Z. Hossain, Phys. Rev. B 81, 125107 (2010).
[8] Yogesh Singh, D. Pal and S. Ramakrishnan, Phys. Rev. B **70**, 064403 (2004).
[9] H. D. Yang, P. Klavins, and R. N. Shelton, Phys. Rev. B

43, 7688 (1991).
[10] K. Ghosh, S. Ramakrishnan, and G. Chandra, Phys. Rev. B 48, 4152 (1993).
[11] S. V. Smaalen, M. Shaz, L. Palatinus, P. Daniels, F. Galli, G. J. Nieuwenhuys, and J. A. Mydosh,Phys. Rev. B **69**, 014103 (2004).
[12] B. Becker, N. G. Patil, S. Ramakrishnan, A. A. Menovsky, G. J. Nieuwenhuys, J. A. Mydosh, M. Kohgi, and K. Iwasa, Phys. Rev. B **59**, 7266 (1999).
[13] Yogesh Singh, Dilip Pal, S. Ramakrishnan, A. M. Awasthi, and S. K. Malik, Phys. Rev. B 71, 045109 (2005).
[14] Y. K. Kuo and K. M. Sivakumar, T. H. Su and C. S. Lue, Phys. Rev. B **74**, 045115 (2006).
[15] N. S. Sangeetha, A. Thamizhavel, C. V Tomy, Saurabh Basu, A. M. Awasthi, S. Ramakrishnan and D. Pal, Phys. Rev. B **86**, 024524 (2012).
[16] Juan Rodriguez-Carvajal, Phys. B (Amsterdam) **55**, 192 (1993).
[17] F. Galli, S. Ramakrishnan, T. Taniguchi, G. J. Nieuwenhuys, J. A. Mydosh, S. Geupe, J. L udecke and S. van Smaalen, Phys. Rev. Lett. **85**, 158 (2000).
[18] J. W. Brill, M. Chung, Y.-K. Kuo, X. Zhan, and E. Figueroa, Phys. Rev. Lett. 74, 1182 (1995).
[19] R. S. Kwok and S. E. Brown, Phys. Rev. Lett. **63**, 895âĂŞ898 (1989).
[20] R. S. Kwok and G. Gruner, S. E. Brown, Phys. Rev. Lett. **65**, 365âĂŞ368 (1990).
[21] S. TomiÄĞ, K. BiljakoviÄĞ, D. Djurek, J.R. Cooper, P. Monceau, A. Meerschaut, Solid State Commun. 38 109 (1981) .
[22] R. A. Craven and S. F. Meyer, Phys. Rev. B **16**, 4583 (1977).
[23] J. L Hodeau, M. Marezio, C. Roucau, R. Ayroles, A. Meerschaut, J. Rouxel and P. Monceau, J. Phys. C: Solid State Phys., **11** (1978).